Title
Source Provenance of Obsidian E Artifacts for Sites along U.S. 491, Navajo Nation, McKinley and San Juan Counties, New Mexico

Author
Shackley, M. Steven

Publication Date
2013-10-25

GEOARCHAEOLOGICAL XRF LAB

GEOARCHAEOLOGICAL X-RAY FLUORESCENCE SPECTROMETRY LABORATORY
8100 Wyoming Blvd., Ste M4-158 Albuquerque, NM 87113
USA

SOURCE PROVENANCE OF OBSIDIAN E ARTIFACTS FOR SITES ALONG U.S. 491, NAVAJO NATION, MCKINLEY AND SAN JUAN COUNTIES, NEW MEXICO

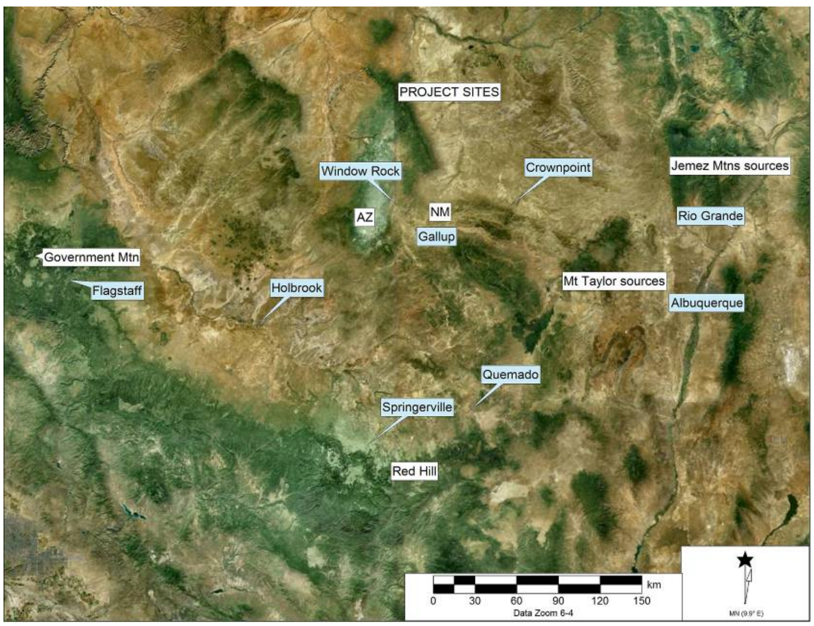

M. Steven Shackley, Ph.D., Director
Geoarchaeological XRF Laboratory
Albuquerque, New Mexico

Report Prepared for

Dr. Bradley Vierra
SRI, Inc.
Albuquerque, New Mexico

25 October 2013

INTRODUCTION

The analysis here of 85 obsidian artifacts from a number of contexts in northwestern New Mexico along U.S. Highway 491 indicates a very diverse procurement of obsidian for the production of stone tools including sources from northern Arizona to southwestern New Mexico, some over 300 km distant. A short discussion of the results is included relevant to the diverse procurement and source assignments.

LABORATORY SAMPLING, ANALYSIS AND INSTRUMENTATION

All archaeological samples are analyzed whole. The results presented here are quantitative in that they are derived from "filtered" intensity values ratioed to the appropriate x-ray continuum regions through a least squares fitting formula rather than plotting the proportions of the net intensities in a ternary system (McCarthy and Schamber 1981; Schamber 1977). Or more essentially, these data through the analysis of international rock standards, allow for inter-instrument comparison with a predictable degree of certainty (Hampel 1984; Shackley 2011a).

All analyses for this study were conducted on a ThermoScientific *Quant'X* EDXRF spectrometer, located at the University of California, Berkeley. It is equipped with a thermoelectrically Peltier cooled solid-state Si(Li) X-ray detector, with a 50 kV, 50 W, ultra-high-flux end window bremsstrahlung, Rh target X-ray tube and a 76 µm (3 mil) beryllium (Be) window (air cooled), that runs on a power supply operating 4-50 kV/0.02-1.0 mA at 0.02 increments. The spectrometer is equipped with a 200 l min^{-1} Edwards vacuum pump, allowing for the analysis of lower-atomic-weight elements between sodium (Na) and titanium (Ti). Data acquisition is accomplished with a pulse processor and an analogue-to-digital converter. Elemental composition is identified with digital filter background removal, least squares empirical peak deconvolution, gross peak intensities and net peak intensities above background.

The analysis for mid Zb condition elements Ti-Nb, Pb, Th, the x-ray tube is operated at 30 kV, using a 0.05 mm (medium) Pd primary beam filter in an air path at 200 seconds livetime to generate x-ray intensity Ka-line data for elements titanium (Ti), manganese (Mn), iron (as $Fe_2O_3^T$), cobalt (Co), nickel (Ni), copper, (Cu), zinc, (Zn), gallium (Ga), rubidium (Rb), strontium (Sr), yttrium (Y), zirconium (Zr), niobium (Nb), lead (Pb), and thorium (Th). Not all these elements are reported since their values in many volcanic rocks are very low. Trace element intensities were converted to concentration estimates by employing a least-squares calibration line ratioed to the Compton scatter established for each element from the analysis of international rock standards certified by the National Institute of Standards and Technology (NIST), the US. Geological Survey (USGS), Canadian Centre for Mineral and Energy Technology, and the Centre de Recherches Pétrographiques et Géochimiques in France (Govindaraju 1994). Line fitting is linear (XML) for all elements but Fe where a derivative fitting is used to improve the fit for iron and thus for all the other elements. When barium (Ba) is analyzed in the High Zb condition, the Rh tube is operated at 50 kV and up to 1.0 mA, ratioed to the bremsstrahlung region (see Davis 2011; Shackley 2011). Further details concerning the petrological choice of these elements in Southwest obsidians is available in Shackley (1988, 1995, 2005; also Mahood and Stimac 1991; and Hughes and Smith 1993). Nineteen specific pressed powder standards are used for the best fit regression calibration for elements Ti-Nb, Pb, Th, and Ba, include G-2 (basalt), AGV-2 (andesite), GSP-2 (granodiorite), SY-2 (syenite), BHVO-2 (hawaiite), STM-1 (syenite), QLO-1 (quartz latite), RGM-1 (obsidian), W-2 (diabase), BIR-1 (basalt), SDC-1 (mica schist), TLM-1 (tonalite), SCO-1 (shale), NOD-A-1 and NOD-P-1 (manganese) all US Geological Survey standards, NIST-278 (obsidian), U.S. National Institute of Standards and Technology, BE-N (basalt) from the Centre de Recherches Pétrographiques et

Géochimiques in France, and JR-1 and JR-2 (obsidian) from the Geological Survey of Japan (Govindaraju 1994).

The data from the WinTrace™ software were translated directly into Excel for Windows software for manipulation and on into SPSS for Windows for statistical analyses. In order to evaluate these quantitative determinations, machine data were compared to measurements of known standards during each run. RGM-1 a USGS obsidian standard was analyzed during the analysis of the obsidian artifacts (Table 1).

Source assignments were made by reference to the laboratory data base (see Shackley 1995, 2005). Further information on the laboratory instrumentation can be found at: http://www.swxrflab.net/. Trace element data exhibited in Table 1 are reported in parts per million (ppm), a quantitative measure by weight (see also Figures 1 through 3).

DISCUSSION

A large assemblage like this requires some interpretation of the statistical results. The majority of artifacts were produced from one of two chemical groups at Mount Taylor, the nearest source to these sites (Tables 1 and 2, Figures 1 and 2). Some explanation is useful.

The Mount Taylor Volcanic Field

The "Grants Ridge" source of archaeological obsidian in the Mount Taylor Volcanic Field in northwestern New Mexico was systematically sampled and analyzed in the 1990s (Shackley 1998, 2005). Previous chemical analyses by Baugh and Nelson (1987) and others have generally been based on grab samples from the East Grants Ridge area. The 1998 study of archaeological obsidian from the Zuni and Hopi areas suggested that, unlike the somewhat vitrophyric glass from Grants Ridge, prehistoric knappers preferred an aphyric glass that while chemically similar, does not elementally covary with samples from Grants Ridge. Systematic survey and sampling resulted in the discovery of another source on Horace Mesa to the east of

East Grants Ridge. These nodules up to 8 cm in diameter are aphyric and are a better medium for tool production. The chemistry differs in a number of incompatibles, but appears to be derived from the same magma source of high silica rhyolite, a late Tertiary and early eruptive phase in the Mount Floyd field (see Goff et al. 2008). A complete major, minor, and trace analysis was completed using the Philips PW2400 WXRF in the lab published in Shackley (1998).

In June and September 2013, La Jara Mesa was sampled on the mesa top and in the road cut and ash flow where Hwy 547 cuts through La Jara Mesa. The distinction between the two mesas is mainly due to a normal fault that separates the two, but this research and that of Goff et. al (2008) indicates that the ash flow on Horace and La Jara mesas are a single unit, now dated to 3.26 ± 0.04 Ma by $Ar^{40/39}$ (Goff et al. 2008). Lipman and Mehnert (1979) dated the East Grants Ridge glass at an unknown locality by K/Ar at 3.34 ± 0.16, potentially older, but statistically similar, given the vagaries of early K/Ar dating. The analysis and plot of Y/Nb indicates this relationship and the distinction between Horace/La Jara mesa and East Grants Ridge obsidian (Figure 1). Again, the obsidian from both Horace and La Jara mesas is generally aphyric as opposed to vitrophyric fabric at East Grants Ridge. The Grants Ridge obsidian, however, is an adequate media for tool production and formal tools including projectile points were produced from this obsidian in prehistory as seen in this assemblage.

Distance to Source

The distance to some of the sources in this assemblage is relatively great indicating some complexity in the social relations at different time periods in these sites; the interpretation of which is up to SRI. The greatest distance is to Government Mountain over 300 km west in the San Francisco Volcanic Field in Arizona (Figure 4). This is a large nodule Quaternary source common in Arizona sites, and while this source has been recovered in New Mexico sites, it is not that common. One expanding stemmed, corner notched point was produced from Government

Mountain and could have entered the site as a complete tool. The next greatest distance to source is Red Hill over 270 km south of these sites in western New Mexico. This is a high quality marekanite source, that while a good media for tool production was not used extensively in the Southwest outside the immediate region in any time period (see Duff et al. 2012; Figures 3 and 4 here). I have not seen Red Hill obsidian this far north in my studies.

The next group of sources distant from these sites are those pre-caldera and caldera event sources in the Jemez Mountains (Bear Springs Peak, El Rechuelos, Cerro Toledo Rhyolite, and Valles Rhyolite) about 200 km east (Figure 3). These are, of course, common in Southwestern sites in all time periods, Valles Rhyolite is indeed distributed throughout North America, particularly in the West (Shackley 2005).

REFERENCES CITED

Baugh, T.G., and Nelson, F.W., Jr.
1987 New Mexico obsidian sources and exchange on the southern Plains. *Journal of Field Archaeology* 14**:**313-329.

Davis, M.K., T.L. Jackson, M.S. Shackley, T. Teague, and J. Hampel
2011 Factors Affecting the Energy-Dispersive X-Ray Fluorescence (EDXRF) Analysis of Archaeological Obsidian. In *X-Ray Fluorescence Spectrometry (XRF) in Geoarchaeology*, edited by M.S. Shackley, pp. 45-64. Springer, New York.

Duff, A.I., J.M. Moss, T.C. Windes, J. Kantner, and M.S. Shackley
2012 Patterning in Procurement of Obsidian in Chaco Canyon and in Chaco-era Communities in New Mexico as Revealed by X-Ray Fluorescence. *Journal of Archaeological Science*, 39:2995-3007.

Goff, F., S.A. Kelley, K. Zeigler, P. Drakos, and C.J. Goff
2008 Preliminary geologic map of the Lobo Springs quadrangle, Cibola County, New Mexico. New Mexico Bureau of Geology and Mineral Resources Open File Geologic Map Series OF-GM-181.

Govindaraju, K.
1994 1994 Compilation of Working Values and Sample Description for 383 Geostandards. *Geostandards Newsletter* 18 (special issue).

Hampel, Joachim H.
1984 Technical Considerations in X-ray Fluorescence Analysis of Obsidian. In *Obsidian Studies in the Great Basin*, edited by R.E. Hughes, pp. 21-25. Contributions of the University of California Archaeological Research Facility 45. Berkeley.

Hildreth, W.
1981 Gradients in Silicic Magma Chambers: Implications for Lithospheric Magmatism. *Journal of Geophysical Research* 86:10153-10192.

Hughes, Richard E., and Robert L. Smith
1993 Archaeology, Geology, and Geochemistry in Obsidian Provenance Studies. *In Scale on Archaeological and Geoscientific Perspectives*, edited by J.K. Stein and A.R. Linse, pp. 79-91. Geological Society of America Special Paper 283.

Lipman, P.W., and Mehnert, H.H.
1979 Potassium-argon ages from the Mount Taylor volcanic field, New Mexico. U.S. Geological Survey Professional Paper 1124-B, 8 pp.

Mahood, Gail A., and James A. Stimac
1990 Trace-Element Partitioning in Pantellerites and Trachytes. *Geochemica et Cosmochimica Acta* 54:2257-2276.

McCarthy, J.J., and F.H. Schamber
1981 Least-Squares Fit with Digital Filter: A Status Report. In *Energy Dispersive X-ray Spectrometry*, edited by K.F.J. Heinrich, D.E. Newbury, R.L. Myklebust, and C.E. Fiori, pp. 273-296. National Bureau of Standards Special Publication 604, Washington, D.C.

Schamber, F.H.
1977 A Modification of the Linear Least-Squares Fitting Method which Provides Continuum Suppression. In *X-ray Fluorescence Analysis of Environmental Samples*, edited by T.G. Dzubay, pp. 241-257. Ann Arbor Science Publishers.

Shackley, M. Steven
1992 The Upper Gila River Gravels as an Archaeological Obsidian Source Region: Implications for Models of Exchange and Interaction. *Geoarchaeology* 7:315-326.

1995 Sources of Archaeological Obsidian in the Greater American Southwest: An Update and Quantitative Analysis. *American Antiquity* 60(3):531-551.

1998 Geochemical Differentiation and Prehistoric Procurement of Obsidian in the Mount Taylor Volcanic Field, Northwest New Mexico. *Journal of Archaeological Science* 25:1073-1082.

2005 *Obsidian: Geology and Archaeology in the North American Southwest*. University of Arizona Press, Tucson.

2011 An Introduction to X-Ray Fluorescence (XRF) Analysis in Archaeology. In *X-Ray Fluorescence Spectrometry (XRF) in Geoarchaeology*, edited by M.S. Shackley, pp. 7-44. Springer, New York.

Table 1. Elemental concentrations and source assignments for the obsidian archaeological specimens and USGS RGM-1 obsidian standard. All measurements in parts per million (ppm).

Sample	Ti	Mn	Fe	Rb	Sr	Y	Zr	Nb	Pb	Th	Source
Q-3-76											
47	621	382	11594	154	11	37	160	50	25	18	Valles Rhy.
99	378	613	12069	515	11	88	130	230	62	33	Horace-La Jara/Mt Taylor
1026	581	388	11783	163	12	43	165	57	26	15	Valles Rhy.
Q-15-43											
127	347	591	11762	545	12	90	139	231	61	32	Horace-La Jara/Mt Taylor
303	675	387	11805	163	12	44	167	54	23	25	Valles Rhy.
610	282	630	11653	530	11	87	130	221	61	30	Horace-La Jara/Mt Taylor
488-1	503	673	10790	515	10	73	98	174	59	16	E Grants Ridge/Mt Taylor
488-2	340	768	11119	574	9	81	108	189	67	28	E Grants Ridge/Mt Taylor
488-3	518	799	11317	571	10	77	107	188	71	29	E Grants Ridge/Mt Taylor
Q-15-29											
20	450	600	10621	174	16	39	68	46	32	19	Red Hill
21	823	583	11597	181	22	38	69	58	36	18	Red Hill
29	811	586	11507	173	17	35	69	50	38	21	Red Hill
74	623	557	12365	209	11	67	174	95	38	23	Cerro Toledo Rhy
114	808	368	11980	155	12	41	155	53	23	21	Valles Rhy.
155	534	479	11797	209	10	62	172	105	35	28	Cerro Toledo Rhy
392	471	594	11623	500	14	87	131	218	58	28	Horace-La Jara/Mt Taylor
607	445	913	11624	554	13	62	92	158	74	28	E Grants Ridge/Mt Taylor
646	602	1292	11339	535	9	80	113	193	63	30	E Grants Ridge/Mt Taylor
652	464	758	12929	570	11	85	127	199	77	21	E Grants Ridge/Mt Taylor
666	443	604	11952	511	10	85	132	220	59	24	Horace-La Jara/Mt Taylor
136-1	542	526	12377	225	9	64	182	98	41	22	Cerro Toledo Rhy
136-2	472	489	11975	206	11	64	177	98	37	27	Cerro Toledo Rhy
289-1	487	844	13355	623	15	93	135	222	79	32	Horace-La Jara/Mt Taylor
289-10	752	577	11438	432	10	70	106	172	50	12	E Grants Ridge/Mt Taylor
289-11	649	726	12527	518	11	77	119	197	61	18	E Grants Ridge/Mt Taylor
289-12	1051	630	11863	450	13	65	102	166	56	26	E Grants Ridge/Mt Taylor
289-13	583	668	1244	533	12	88	127	211	63	26	Horace-La Jara/Mt

			3								Taylor
289-14	688	692	12400	535	10	78	122	200	63	31	E Grants Ridge/Mt Taylor
289-15	732	651	12234	565	12	84	123	203	65	24	E Grants Ridge/Mt Taylor
289-2	734	611	11878	518	14	80	119	197	58	31	E Grants Ridge/Mt Taylor
289-3	605	578	11895	475	13	80	124	198	52	27	E Grants Ridge/Mt Taylor
289-4	482	613	11802	531	13	86	115	191	57	28	E Grants Ridge/Mt Taylor
289-5	892	499	10990	390	11	67	100	166	44	17	E Grants Ridge/Mt Taylor
289-6	710	586	11628	491	11	81	125	200	57	28	E Grants Ridge/Mt Taylor
289-7	886	760	12725	491	12	66	106	171	70	41	E Grants Ridge/Mt Taylor
289-8	938	687	12552	493	12	72	111	172	63	32	E Grants Ridge/Mt Taylor
289-9	700	583	11634	465	9	75	115	185	55	24	E Grants Ridge/Mt Taylor
329-1	1040	627	11817	428	12	61	95	148	52	9	E Grants Ridge/Mt Taylor
329-2	647	756	12675	522	12	70	116	187	63	32	E Grants Ridge/Mt Taylor
632-1	430	572	11570	491	11	83	130	216	53	19	Horace-La Jara/Mt Taylor
632-2	398	537	11525	488	12	81	123	209	53	30	Horace-La Jara/Mt Taylor
693-1	381	615	11583	519	12	91	134	228	59	34	Horace-La Jara/Mt Taylor
693-2	1021	723	13152	488	13	68	114	171	63	24	E Grants Ridge/Mt Taylor
693-3	524	583	11704	512	13	93	136	226	60	35	Horace-La Jara/Mt Taylor
693-4	352	571	11486	503	12	88	131	227	57	24	Horace-La Jara/Mt Taylor
703-1	315	752	11008	563	10	80	110	201	63	25	E Grants Ridge/Mt Taylor
Sample	Ti	Mn	Fe	Rb	Sr	Y	Zr	Nb	Pb	Th	Source
703-2	433	749	11122	546	10	75	112	187	63	20	E Grants Ridge/Mt Taylor
703-3	329	698	10725	524	13	71	107	189	59	27	E Grants Ridge/Mt Taylor
703-4	354	713	10846	541	10	80	106	186	60	28	E Grants Ridge/Mt Taylor
703-5	331	741	10957	560	8	75	115	191	66	20	E Grants Ridge/Mt Taylor
703-6	329	675	10714	526	10	77	108	190	61	25	E Grants Ridge/Mt Taylor
703-8	354	818	11362	602	12	82	121	216	66	28	Horace-La Jara/Mt Taylor
0A0035E86	485	527	10540	170	18	35	67	48	34	16	Red Hill
0A003488E	480	579	11478	502	13	85	125	213	52	33	Horace/Lajara/Mt Taylor
Q-15-28											
0A0032568	667	363	10149	105	39	21	97	52	15	26	Bear Springs Pk
0A0031FB8	843	421	10790	123	44	21	100	50	24	26	Bear Springs Pk
0A0035DFQ	673	354	1031	106	39	17	90	49	22	27	Bear Springs Pk

			2								
Q-15-46											
0A00357E0	353	471	11246	108	81	17	80	52	32	18	Government Mtn
0A0035B1D	656	379	11844	164	11	41	164	52	25	17	Valles Rhy.
0A002577E	589	415	11863	164	11	45	164	53	24	19	Valles Rhy.
0A0025785	682	390	10195	151	12	20	67	46	27	20	El Rechuelos
0A0034E77	663	387	11784	161	13	44	159	51	25	16	Valles Rhy.
0A0034E7C	708	408	11860	160	12	41	154	53	24	18	Valles Rhy.
0A0029B21	577	397	11754	154	11	45	156	53	25	27	Valles Rhy.
0A002578C	612	358	9955	144	12	24	66	43	21	18	El Rechuelos
0A0025637	657	571	12714	230	8	66	182	99	42	25	Cerro Toledo Rhy
0A0035A47	626	396	11844	169	11	48	166	56	27	16	Valles Rhy.
0A0025790	463	483	11324	103	80	23	75	55	29	9	Government Mtn
0A0035AD2	627	419	12045	166	13	48	164	56	28	22	Valles Rhy.
0A0035757	600	330	11139	147	24	43	154	55	23	19	Valles Rhy.
0A00328A0	569	400	11578	161	14	43	162	54	24	16	Valles Rhy.
0A0035719	535	541	11204	453	11	73	112	192	52	18	E Grants Ridge/Mt Taylor
Q-15-52											
0A00354A4	441	806	12879	601	14	95	136	224	78	34	Horace-La Jara/Mt Taylor
Q-15-51											
0A0021510	310	617	11689	522	13	91	138	244	61	28	Horace-La Jara/Mt Taylor
0A0034CFD	372	552	11364	497	10	88	131	225	58	31	Horace-La Jara/Mt Taylor
0A0034E9A	849	574	12724	493	14	85	132	229	56	28	Horace-La Jara/Mt Taylor
Q-15-73											
0A00351FA	774	684	13994	239	8	65	167	90	47	22	Cerro Toledo Rhy
0A0035276	1170	735	14516	249	8	62	170	93	50	32	Cerro Toledo Rhy
0A0035261	927	519	12654	195	8	52	145	74	35	22	Cerro Toledo Rhy
0A0035284	721	390	12137	164	13	42	160	52	25	21	Valles Rhy.
0A0035228	934	556	13003	224	11	65	176	97	40	33	Cerro Toledo Rhy
0A0035245	796	487	12417	204	10	62	167	93	36	31	Cerro Toledo Rhy
0A001A69D	560	524	12287	221	8	67	173	98	38	26	Cerro Toledo Rhy
0A001A669	601	359	9987	145	13	22	66	46	26	17	El Rechuelos
0A001A697	713	555	12597	218	11	68	182	100	38	25	Cerro Toledo Rhy
RGM1-S4	1683	294	13730	149	107	27	216	7	17	12	standard

RGM1-S4	1576	298	13710	150	111	22	216	9	22	19	standard
RGM1-S4	1557	283	13661	151	105	22	215	9	20	11	standard
RGM1-S4	1539	283	13767	150	107	26	219	5	21	16	standard
RGM1-S4	1670	271	13746	152	108	22	220	8	20	15	standard

Table 2. Crosstabulation of site by source.

			Site								
			Q-15-28	Q-15-29	Q-15-43	Q-15-46	Q-15-51	Q-15-52	Q-15-73	Q-3-76	Total
Source	Bear Springs Pk	Count	3	0	0	0	0	0	0	0	3
		% within Source	100.0%	0.0%	0.0%	0.0%	0.0%	0.0%	0.0%	0.0%	100.0%
		% within Sample	100.0%	0.0%	0.0%	0.0%	0.0%	0.0%	0.0%	0.0%	3.5%
		% of Total	3.5%	0.0%	0.0%	0.0%	0.0%	0.0%	0.0%	0.0%	3.5%
	Cerro Toledo Rhy	Count	0	4	0	1	0	0	7	0	12
		% within Source	0.0%	33.3%	0.0%	8.3%	0.0%	0.0%	58.3%	0.0%	100.0%
		% within Sample	0.0%	8.9%	0.0%	6.7%	0.0%	0.0%	77.8%	0.0%	14.1%
		% of Total	0.0%	4.7%	0.0%	1.2%	0.0%	0.0%	8.2%	0.0%	14.1%
	El Rechuelos	Count	0	0	0	2	0	0	1	0	3
		% within Source	0.0%	0.0%	0.0%	66.7%	0.0%	0.0%	33.3%	0.0%	100.0%
		% within Sample	0.0%	0.0%	0.0%	13.3%	0.0%	0.0%	11.1%	0.0%	3.5%
		% of Total	0.0%	0.0%	0.0%	2.4%	0.0%	0.0%	1.2%	0.0%	3.5%
	Valles Rhy.	Count	0	1	1	9	0	0	1	2	14
		% within Source	0.0%	7.1%	7.1%	64.3%	0.0%	0.0%	7.1%	14.3%	100.0%
		% within Sample	0.0%	2.2%	16.7%	60.0%	0.0%	0.0%	11.1%	66.7%	16.5%
		% of Total	0.0%	1.2%	1.2%	10.6%	0.0%	0.0%	1.2%	2.4%	16.5%
	E Grants Ridge/Mt Taylor	Count	0	25	3	1	0	0	0	0	29
		% within Source	0.0%	86.2%	10.3%	3.4%	0.0%	0.0%	0.0%	0.0%	100.0%
		% within Sample	0.0%	55.6%	50.0%	6.7%	0.0%	0.0%	0.0%	0.0%	34.1%
		% of Total	0.0%	29.4%	3.5%	1.2%	0.0%	0.0%	0.0%	0.0%	34.1%
	Horace-La Jara/Mt Taylor	Count	0	11	2	0	3	1	0	1	18
		% within Source	0.0%	61.1%	11.1%	0.0%	16.7%	5.6%	0.0%	5.6%	100.0%
		% within Sample	0.0%	24.4%	33.3%	0.0%	100.0%	100.0%	0.0%	33.3%	21.2%
		% of Total	0.0%	12.9%	2.4%	0.0%	3.5%	1.2%	0.0%	1.2%	21.2%
	Government Mtn	Count	0	0	0	2	0	0	0	0	2
		% within Source	0.0%	0.0%	0.0%	100.0%	0.0%	0.0%	0.0%	0.0%	100.0%
		% within Sample	0.0%	0.0%	0.0%	13.3%	0.0%	0.0%	0.0%	0.0%	2.4%
		% of Total	0.0%	0.0%	0.0%	2.4%	0.0%	0.0%	0.0%	0.0%	2.4%
	Red Hill	Count	0	4	0	0	0	0	0	0	4
		% within Source	0.0%	100.0%	0.0%	0.0%	0.0%	0.0%	0.0%	0.0%	100.0%
		% within Sample	0.0%	8.9%	0.0%	0.0%	0.0%	0.0%	0.0%	0.0%	4.7%
		% of Total	0.0%	4.7%	0.0%	0.0%	0.0%	0.0%	0.0%	0.0%	4.7%
Total		Count	3	45	6	15	3	1	9	3	85
		% within Source	3.5%	52.9%	7.1%	17.6%	3.5%	1.2%	10.6%	3.5%	100.0%
		% within Sample	100.0%	100.0%	100.0%	100.0%	100.0%	100.0%	100.0%	100.0%	100.0%
		% of Total	3.5%	52.9%	7.1%	17.6%	3.5%	1.2%	10.6%	3.5%	100.0%

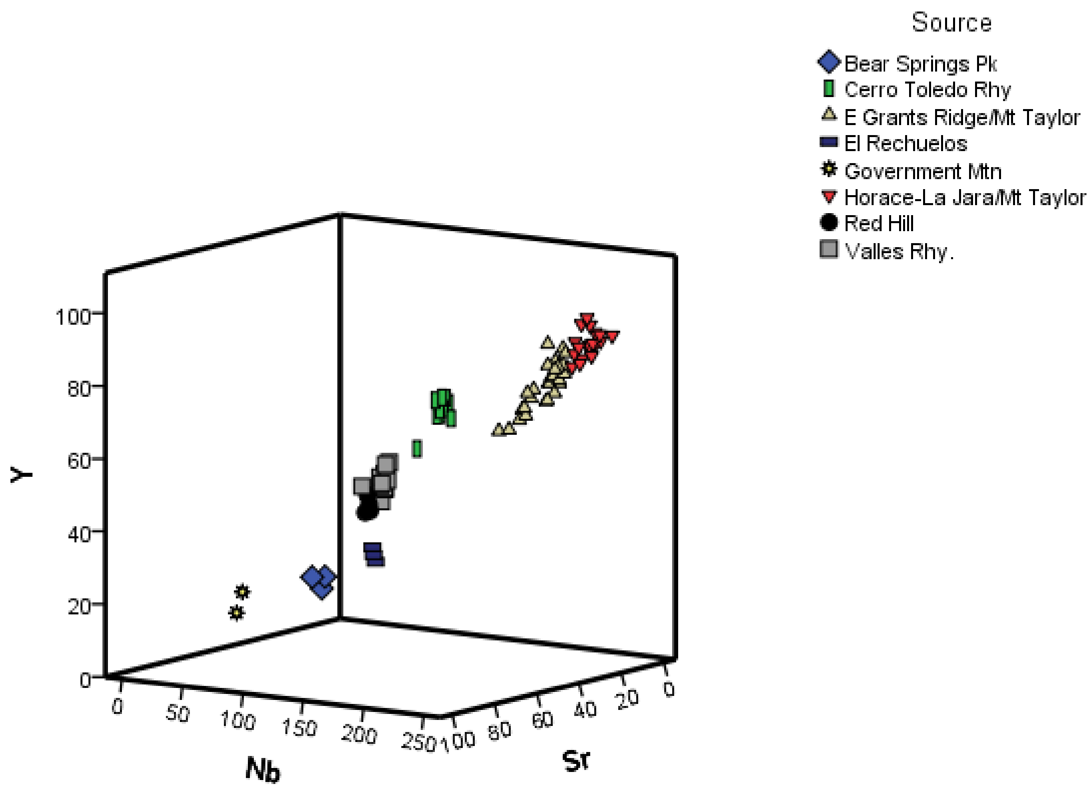

Figure 1. Nb, Y, Sr three-dimensional plot of the elemental concentrations for all the obsidian archaeological specimens. Further discrimination below.

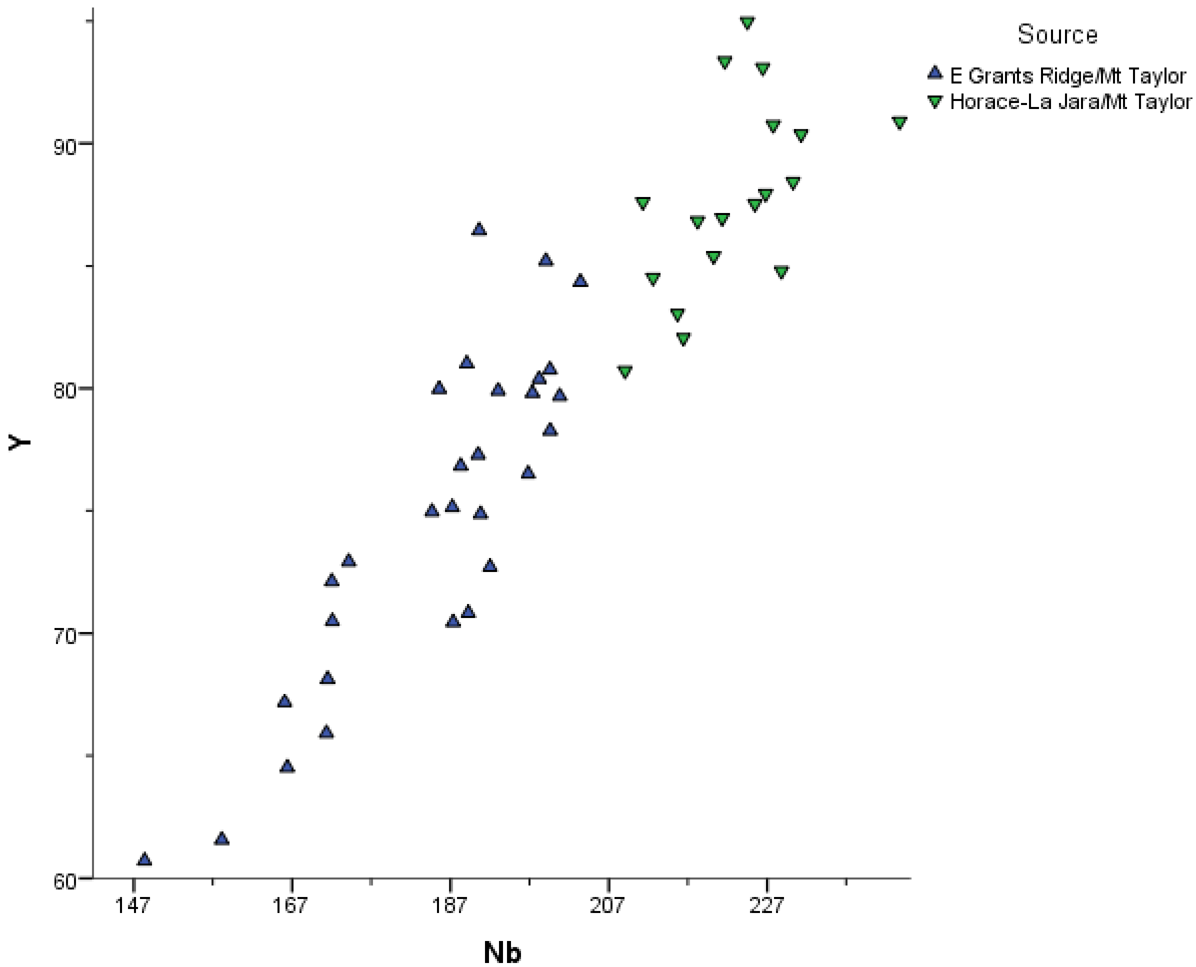

Figure 2. Nb versus Y bivariate plot of the Mount Taylor chemical groups. Seeming overlap due to small sample sizes of some artifacts (see Davis et al. 2012).

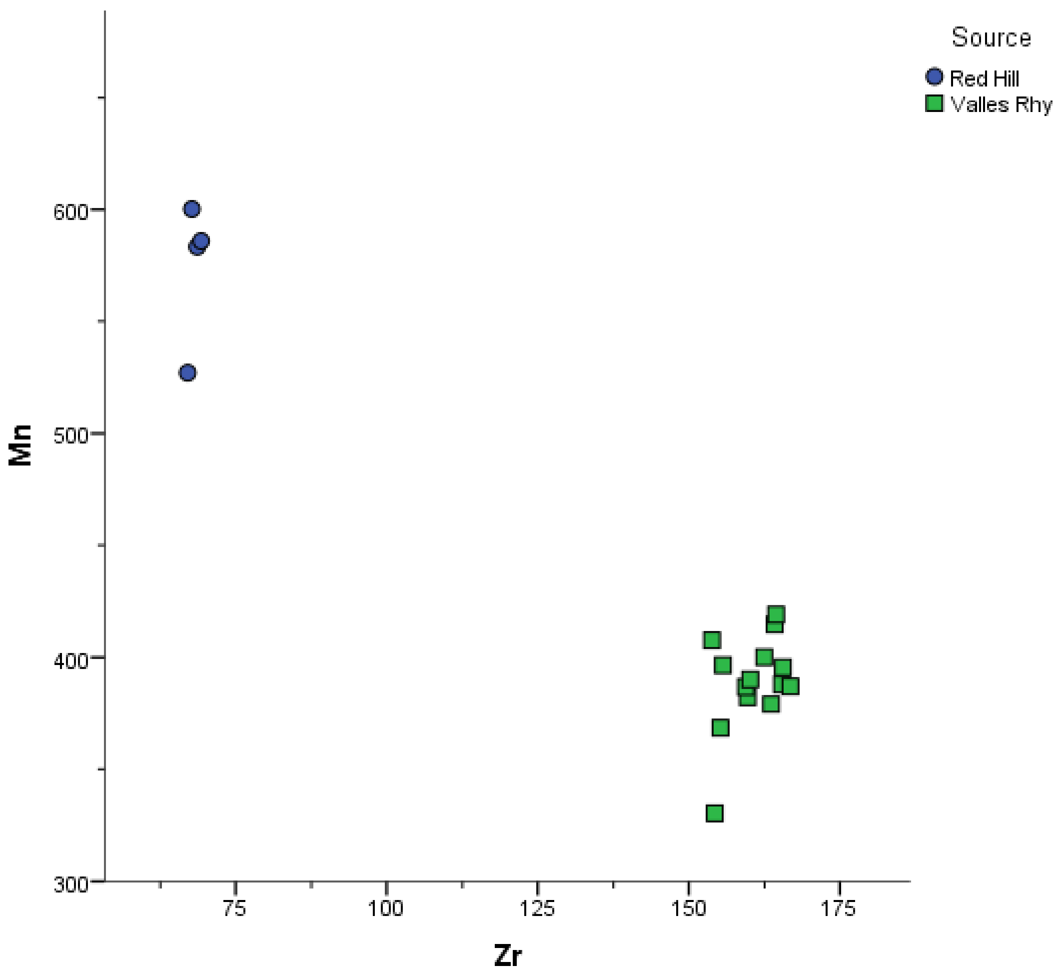

Figure 3. Zr versus Mn bivarite plot of the Valles Rhyolite and Red Hill assigned artifacts providing discriminating clarity.

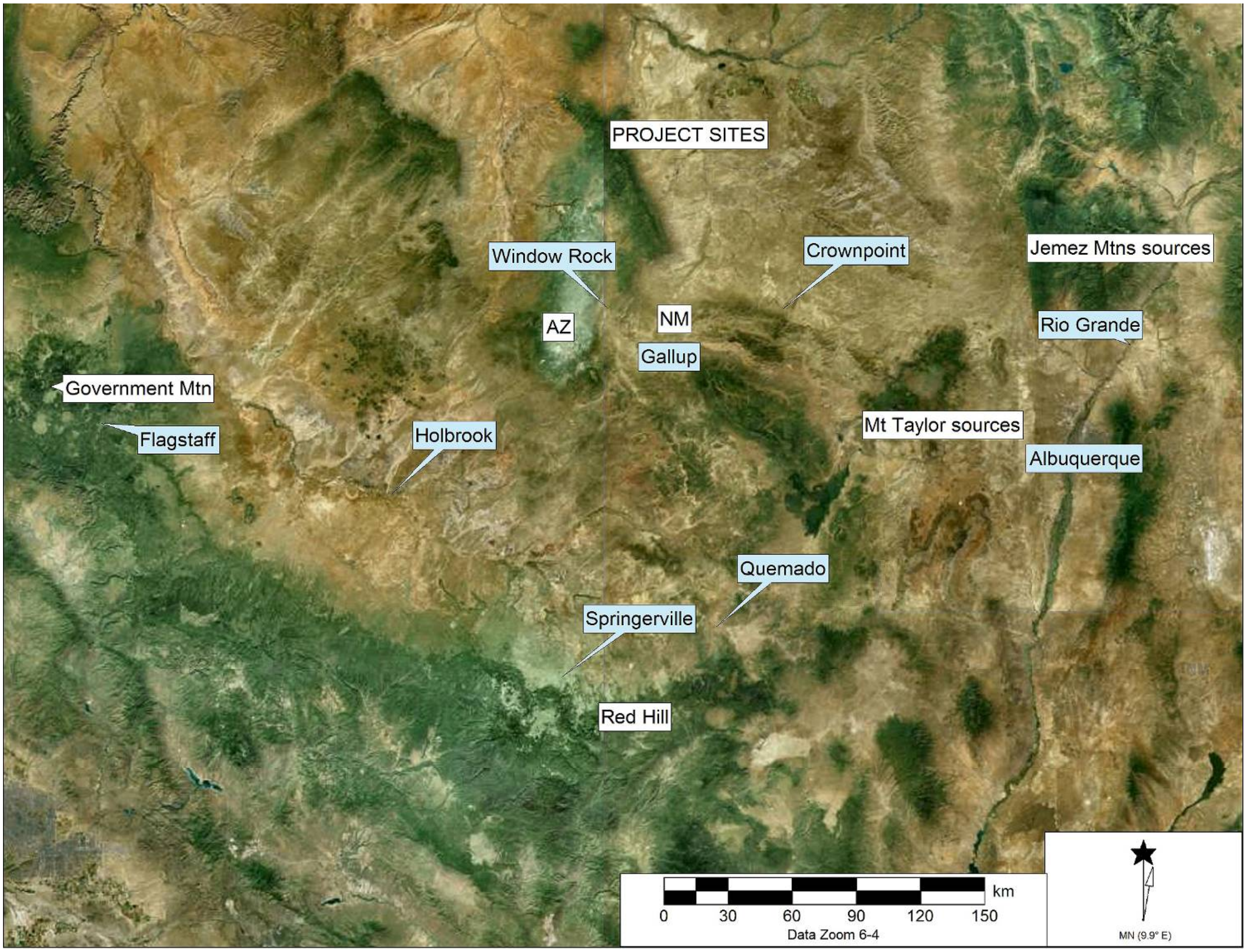

Figure 4. Digital elevation model of showing site location, source locations, and appropriate features.